frontiers in Materials

REVIEW
published: 18 March 2022
doi: 10.3389/fmats.2022.857385

Research Advance in Manganese Nanoparticles in Cancer Diagnosis and Therapy

*Dengyun Nie[1], Yinxing Zhu[1], Ting Guo[2], Miao Yue[1] and Mei Lin[2,3]**

[1]Nanjing University of Chinese Medicine, Nanjing, China, [2]Clinical Laboratory of Taizhou People's Hospital Affiliated to Nanjing Medical University, Taizhou, China, [3]Clinical Laboratory, Taizhou People's Hospital Affiliated to Nanjing University of Chinese Medicine, Taizhou, China

As the second reason of causing death after cardiovascular disease for human being, cancer is damaging people all over the world. Fortunately, rapidly developing in the past decade, nanotechnology has become one of the most promising technologies for cancer theranostics. Recent studies have demonstrated that metal nanoparticles, especially manganese nanoparticles (Mn-NPs), exhibit amazing potential for application in multifarious oncology fields according to their characteristic fundamental properties. Although global scientists have developed a variety of new Mn-NPs and have proved their preponderance in cancer diagnosis and treatment, Mn-NPs are still not approved for clinical use. In this paper, the recent research progress of Mn-NPs in the fields of cancer diagnosis and therapy is reviewed. Besides, the future prospect and challenges of Mn-NPs are discussed to explore wider applications of Mn-NPs in clinic. Here, we hope that this review will show a better overall understanding of Mn-NPs and provide guidance for their design in clinical applications for cancer.

Keywords: cancer, diagnosis, therapy, manganese, nanoparticles

OPEN ACCESS

Edited by:
Jinbing Xie,
Southeast University, China

Reviewed by:
Eunsoo Yoo,
North Carolina Agricultural and Technical State University, United States
Xianglong Hu,
South China Normal University, China

****Correspondence:***
Mei Lin
l_mei@163.com

Specialty section:
This article was submitted to Biomaterials, a section of the journal Frontiers in Materials

Received: *18 January 2022*
Accepted: *04 March 2022*
Published: *18 March 2022*

Citation:
Nie D, Zhu Y, Guo T, Yue M and Lin M (2022) Research Advance in Manganese Nanoparticles in Cancer Diagnosis and Therapy. Front. Mater. 9:857385. doi: 10.3389/fmats.2022.857385

1 INTRODUCTION

Cancer, a morbid state caused by aberrant cell proliferation, is the second leading cause of death globally. Cancer caused almost ten million deaths in 2020 on the basis of data released by the World Health Organization (WHO), and unfortunately the incidence of cancer is still rising year by year (Siegel et al., 2021). Cancer is undoubtedly a major risk to the health and lives of people in the world. Molecular imaging technology has high veracity and dependability in elucidating biological processes and monitoring disease status, and particularly has important value in tumor detection and prognosis monitoring. The main types of cancer therapy include surgery, chemotherapy, radiotherapy, immunotherapy and so on. However, current imaging techniques have their own limitations of applications in clinical cases and traditional treatments are accompanied by diverse side effects. Therefore, it is desirable to develop a better medical strategy for diagnosis and treatments of cancer. In recent years, the rapid development of nanomedicine seems to be a promising option to overcome these challenges of cancer.

A series of nanoparticles (NPs) have been developed and increasingly entered the stage of clinical application (Kim et al., 2010; Baetke et al., 2015). Among them, manganese nanoparticles (Mn-NPs) show good biocompatibility and low side effects because manganese (Mn) is a basic building of cells and a cofactor for many metabolic enzymes (Felton et al., 2014). Thus, a considerable number of researches have been conducted, focusing on the development of Mn-NPs and their potential

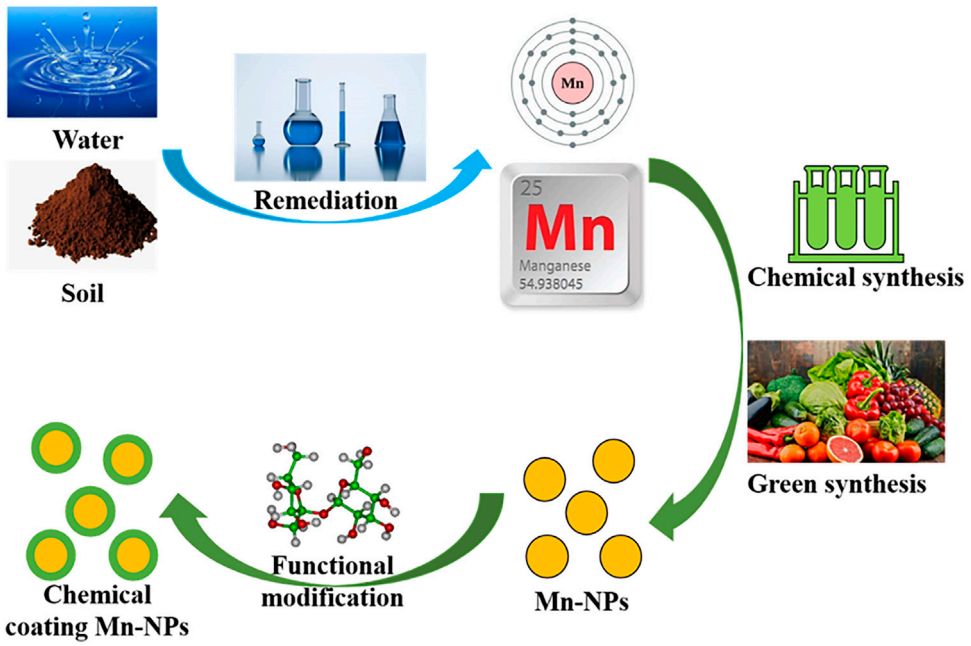

FIGURE 1 | Source and synthesis of Mn-NPs.

applications in multipurpose diagnosis and therapy of cancer. Herein, we provide a review of the studies that have been conducted on Mn-NPs over the past decade, describe the synthesis and surface functionalization of Mn-NPs as well as the use of Mn-NPs in cancer diagnosis and treatments in detail, and briefly discuss the possible molecular mechanisms underlying cancer.

2 CLASSIFICATION AND SYNTHESIS

Mn as the third most abundant transition metal on earth can be prepared into various Mn nanostructures through different nanotechnologies, such as NPs, nanorods, nanobelts, nanosheets, nanowires, nanotubes, nanofibers and other hierarchical structures. Thereinto, Mn-NPs are divided into two main categories: Mn oxide NPs and Mn-doped NPs, and their preparation methods are not universal due to their customization and complexity of configurations. Although a brief overview of the synthesis of MnO_2 NPs, which are the simplest Mn-NPs, will be described here for an instance, readers are encouraged to view other reviews to obtain detailed information about the synthesis of other kinds of Mn-NPs. A representative synthesis procedure of MnO_2 NPs is as follows: 60 ml of saturated argon aqueous solution containing 0.1 mM $KMnO_4$ in a glass container is irradiated in a water bath, and the temperature of the water bath is maintained at 20°C using a cold water circulation system. The container is installed in a constant position and closed from air during the irradiation (Abulizi et al., 2014). Besides, green synthesis of Mn-NPs has received great attention in recent years, which is a new evolved means from the nanobiotechnology and is the latest available method to manufacture Mn-NPs combining materialogy and biotechnology (**Figure 1**) (Hoseinpour and Ghaemi, 2018). Green synthesis of Mn-NPs using raw materials, vegetables and fruits, plant extracts, microorganisms and fungi has advantages of non-toxic, environmentally friendly, clean and low-cost, and it can be completed at room temperature and normal pressure (Singh et al., 2016; Ahmed et al., 2017). Using genetic engineering, molecular cloning, plant extracts and other biotechnologies to green synthesize Mn-NPs with controllable shape and size will be a major advancement in the nanobiotechnology, and how to achieve this achievement is also a huge challenge.

3 CHARACTERISTICS AND MODIFICATION

Mn shows efficient redox performance because it has different oxidation states, ranging from −3 to +7, and has ability to form compounds with a coordination number up to 7.5 (Haque et al., 2021), which led to the use of high oxidation-state Mn species as strong oxidants (Li and Yang, 2018). Mn is effective in improving the catalytic activity in several oxidation reactions. Mn^{2+} can trigger Fenton reaction that converts overexpressed endogenous hydrogen peroxide (H_2O_2) (100 μM~1 mM) (An et al., 2020) into highly toxic reactive oxygen species (ROS) in the acidic tumor microenvironment (TME) at pH 6.5~7.0 (Qian et al., 2019; Anderson and Simon, 2020). Also, Mn in the form of oxides possesses strong redox property and surface nanoarchitectures property. Therefore, Mn-NPs show oxidase-like features for their catalytic properties (Liu et al., 2012), and are widely used in cancer diagnosis and therapy. The activity of Mn-NPs is dependent on their size, morphology, surface area and redox functions (Haque et al.,

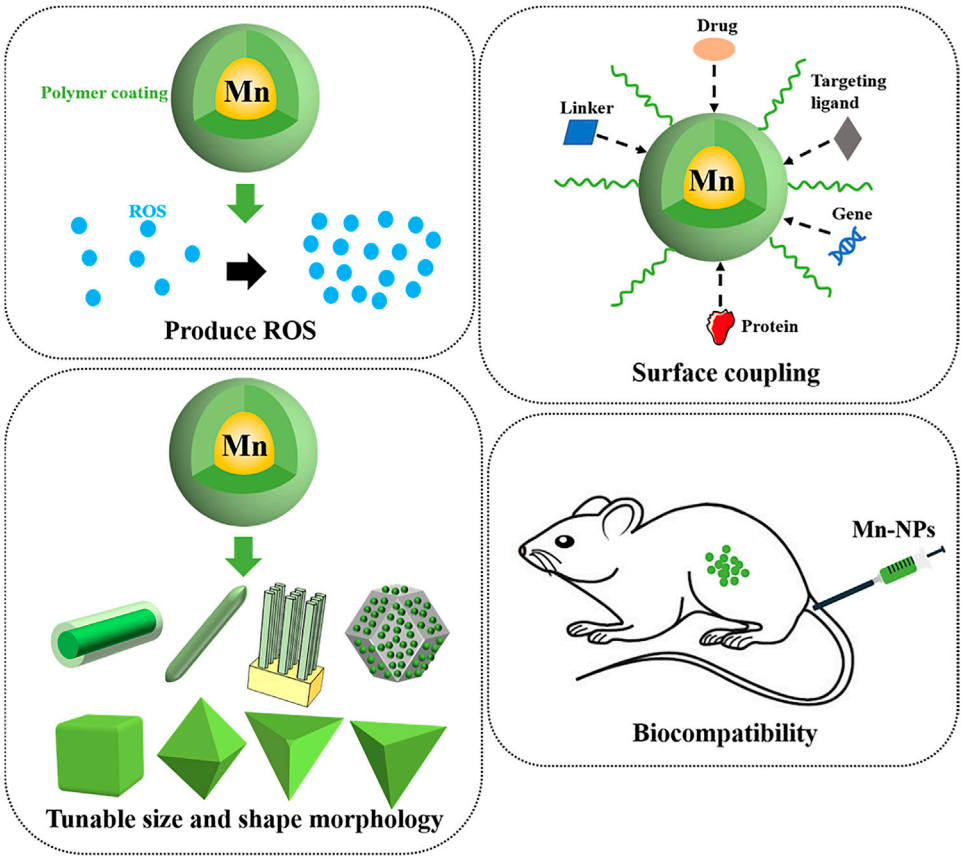

FIGURE 2 | Important properties of Mn-NPs.

2021). Mn-NPs with the diameter ≤100 nm generally exhibit great chemical and physical properties due to fundamental properties of their main part (Mn) and are being used in drug delivery studies owing to their large surface to volume ratio, which can increase the sensitivity to TME. In addition, Mn-NPs have advantages of good biocompatibility and environmental compatibility, high specific capacitance, strong adsorption property and so on.

The negative charge on the surface of Mn-NPs makes them easy to couple, which means that they can be functionalized easily by adding diversified biomolecules such as drugs, targeting ligands, protein, genes and more. Additionally, different kinds of coating provide surface chemistry that facilitates the integration of functional ligands (**Figure 2**). Surface chemical modification contributes to the versatility of Mn-NPs, such as combined treatment of multimodal imaging and chemotherapy-drug delivery (Xi et al., 2017; Yuan et al., 2019).

4 CYTOTOXICITY

Mn is non-toxic metal, so Mn-NPs are also less-toxic materials than other NPs-based compounds, such as various chalcogenides (Hoseinpour and Ghaemi, 2018). Razumov et al. tested toxicity of different kinds of Mn-NPs against glioblastoma U-87MG and U-251 cells and normal human cells and confirmed that Mn oxide NPs exhibited low cytotoxicity (Razumov et al., 2017). Furthermore, Mn-doped NPs also exhibited low cytotoxicity. Islam et al. examined the cytotoxicity of polysaccharide chitosan (CS)-coated Mn ferrite NPs ($MnFe_2O_4$-NPs) in HeLa cells cultured to a confluent state, and found that the cells' survival was 100% and 95% in the absence and presence of these NPs after 24 h incubation, respectively. Thus, no cytotoxic effect was visibly observed for $MnFe_2O_4$ NPs *in vitro* (Islam et al., 2020). However, Mn in the form of complexus still had certain weaknesses *in vivo* such as short blood circulation time and accumulation in the brain (Bellusci et al., 2014), leading to damage to the central nervous system followed by cognitive and movement abnormalities in a few animal models (Sárközi et al., 2009; Oszlánczi et al., 2010; Li et al., 2014; Haque et al., 2021). Bellusci et al. discovered complete clearance of $MnFe_2O_4$ NPs in the kidneys, spleen and brain of mice at day 7. Fortunately, there was no evidence of irreversible histopathological damage to any of the organs examined (Bellusci et al., 2014). Sarkozi et al. reported that rats were injected with a nanosuspension of MnO_2 with approximately 23 nm nominal particle diameter at doses of

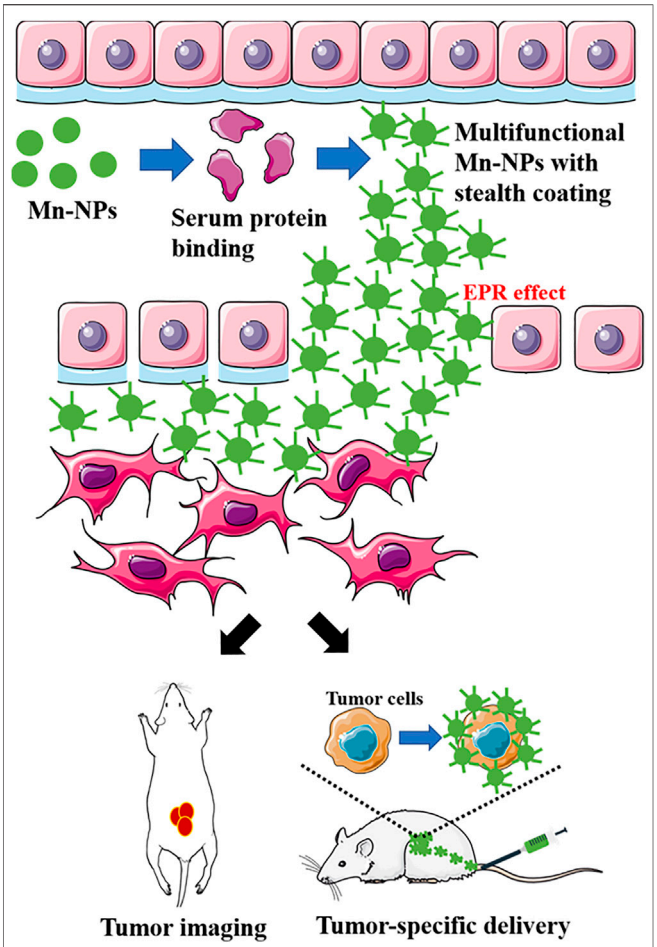

FIGURE 3 | Different approaches of Mn-NPs in cancer diagnosis and treatment.

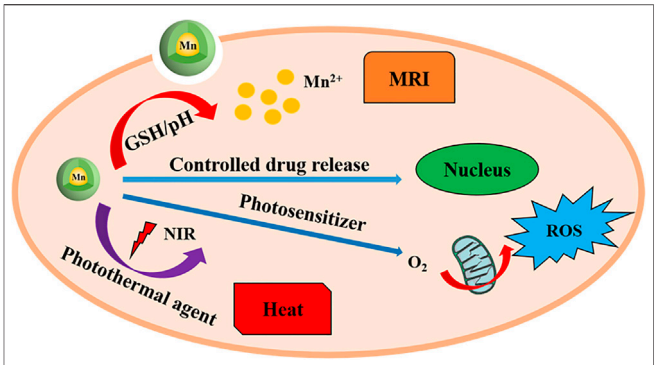

FIGURE 4 | The mechanism of Mn-NPs-based nanotheranostic agents for imaging guided chemotherapy/PDT/PTT and tumor MR imaging.

2.63 and 5.26 mg Mn/kg into the trachea for 3, 6 and 9 weeks. Mn could be examined in their lung and brain samples after treatment. In the open field activity, the proportion of walking and rearing decreased, while the proportion of local activity and inactivity increased. The evoked potential latency was prolonged, and the tail nerve conduction velocity was decreased. These results suggested that the Mn content of perfused NPs could enter the brain through the airway, causing nerve damage and reducing exercise capacity (Sárközi et al., 2009). The biocompatibility and non-toxic properties of Mn-NPs make them an all-right option for biomedical applications. Nevertheless, Mn-NPs have cytotoxicity properties against tumor cells (Al-Fahdawi et al., 2015), which is especially beneficial to their applications for cancer diagnosis and therapy.

5 DIFFERENT APPLICATIONS IN CANCER DIAGNOSIS AND THERAPY

Tumor tissue generally has a leaky vasculature, which allows Mn-NPs to accumulate at tumor site easily. This is referred to as the enhanced permeation and retention (EPR) effect of Mn-NPs. Incubation of polymeric Mn-NPs in plasma or serum could result in surface enrichment with multifunctional proteins. The targeting ligands of tumor specific biomarkers were conjugated on to Mn-NPs with the opsonization of serum protein to interact with receptors on the tumor cells, allowing for endocytosis and subsequent release of the drug (Moghimi and Szebeni, 2003). For instance, folic acid (FA) receptors are highly expressed on the surface of liver cancer cells and breast cancer cells (Law et al., 2020; Tao Gong et al., 2021), so the targeted uptake of tumor cells can be achieved by FA-modified Mn-NPs. Mn-NPs have been studied to be used for a great diversity of biomedical applications in cancer diagnosis and treatment based on their above properties (**Figure 3**), such as magnetic resonance imaging, positron emission tomography, chemotherapy, radiotherapy, all of which are discussed in the following subsections.

5.1 Diagnosis

The cancer has a recognizable latent or early asymptomatic stage. A large number of clinical practices have proved that the key to the prognosis of malignant tumors is whether early detection and diagnosis can be achieved so as to take corresponding treatment measures. A shorter interval between diagnoses may contribute to improve five-year survivals in five common cancers (Tørring et al., 2013). Various medical imaging techniques have played an important role in the early detection and diagnosis of cancer for their convenient and precise diagnostic capabilities at the systemic, molecular, and cellular levels, such as magnetic resonance imaging (MRI), positron emission tomography (PET), photoacoustic imaging (PAI) and fluorescence imaging (FI) (**Figure 4**) (Zanzonico, 2019). In this part, we make a detailed introduction of Mn-NPs as contrast agents (CAs) for above imaging techniques.

5.1.1 Magnetic Resonance Imaging

Magnetic resonance imaging (MRI) is a non-invasive detection technique based on the principle of nuclear spins, which is of great value in the clinical diagnosis of cancer. However, most contrast agents used in MRI are nonspecific and fast-excretory, and only can act extracellularly with localization imaging of

tumor cells (Fan et al., 2020). The logical design of theranostic nanoparticles shows synergistic turn-on of therapeutic potency and enhanced diagnostic imaging in response to TME (Hu et al., 2015). Mn was one of the earliest reported paramagnetic contrast materials for MRI based on its potent positive contrast enhancement. The increased accessibility of Mn centers to adjacent water molecules due to the porous architecture of Mn-NPs greatly enhances the contrast capacity of T1-weighted MRI, thus Mn-NPs appear to be a potential choice for MRI tool exploration. Among them, a variety of Mn oxide NPs, such as MnO, MnO_2, Mn_3O_4, and MnO_x NPs have been extensively researched as T1-weighted MRI CAs owing to the short cycle time of Mn^{2+} chelate and the size-controlled cycle time of colloidal NPs(Cai et al., 2019). The high loading content of Mn^{2+} chelate helps Mn-NPs exert a better effect in MRI (Liu et al., 2015). For instance, Yang et al. reported that Mn dioxide on silk fibroin NPs (SF@MnO_2-NPs) could significantly enhance water proton relaxation and improve MRI contrast (Yang et al., 2019).

In order to further improve imaging contrast sensitivity, various Mn-doped NPs as T1- or T2-MRI CAs have been developed (Zhao et al., 2018). Kuo et al. developed gadolinium-Mn-doped magnetism-engineered iron oxide NPs (Gd-MnMEIO-NPs) as a novel contrast agent with enhancement effects in both T1- and T2-weighted MRI of liver with high relaxivity r1 and r2 values. The average hydrodynamic size of Gd-MnMEIO-NPs was 20 nm, and the zeta potential was close to 0 mV, which could effectively avoid their removal from the reticuloendothelial system and prolong their residence time. Gd-MnMEIO-NPs could not only enhance normal liver and living tumor tissues but also improve the visualization of vascular trees. Haemodynamic information from dynamic contrast-enhanced T1-weighted MRI images using Gd-MnMEIO-NPs was helpful to diagnose liver tumors (Kuo et al., 2016).

Prussian blue (PB) as a clinically applied drug has drawn extensive attention in the theranostics of cancer, such as MRI (Dacarro et al., 2018), so PB NPs doped with Mn seemed to display a great performance in the CAs of MRI (Zhu et al., 2015). Then, diversiform multifunctional Mn-doped PB NPs were developed and researched universally, and they all had peculiar longitudinal nuclear MRI relaxivity values (Ali et al., 2018; Gao et al., 2020). Dumont et al. synthesized Mn-containing PB NPs (MnPB-NPs) as CAs for molecular MRI of pediatric brain tumors. The surfaces of these NPs were modified with biotinylated antibodies targeting neuron-glial antigen 2 or biotinylated transferrin which were protein markers overexpressed in pediatric brain tumors. These NPs showed great capacity in MRI quality of pediatric brain tumors *in vitro* (Dumont et al., 2014). These show that Mn-NPs have been widely applicated in the MRI of cancer.

5.1.2 Positron Emission Tomography Imaging

Positron emission tomography (PET) is a reversely progressive clinical imaging technology based on positrons released after decay of positron radionuclides (Fan et al., 2020), which is especially appropriate for early diagnosis of cancers (Tarkin et al., 2020). Combinations of different imaging modalities may be the great trend of future clinical diagnosis, because each of imaging technique has its own unique advantages and limitations in terms of spatial and temporal resolution, tissue penetration depth, detection sensitivity and veracity, and convenience and cost. In this regard, the integration of PET and MRI is developing rapidly and is currently in clinical trials for cancer detection and diagnosis owing to the extremely high sensitivity of PET and the ultra-high spatial resolution of MRI. Mn oxide NPs as a class of typical Mn-NPs, which seemingly have excellent potency as CAs of PET/MRI, are successfully developed and updated in recent years. Likewise, Zhan et al. reported that Mn_3O_4-NPs with conjugation to the anti-CD105 antibody TRC105 and radionuclide copper-64 (^{64}Cu-NOTA-Mn_3O_4@PEG-TRC105-NPs) had excellent specific targeting the vascular marker CD105, and were successfully used in PET/MRI of breast tumors *in vivo* (Zhan et al., 2017). Zhan et al. also synthesized copper-64 labeling of Mn_3O_4-NPs (^{64}Cu-NOTA-FA-FI-PEG-PEI-Ac-Mn_3O_4-NPs) and resoundingly put them into applications for PET/MRI of human cervical cancer xenografts which overexpress folate receptor in mice (Zhu et al., 2018). Otherwise, Shi et al. developed Mn ferrite NPs conjugated with integrin $\alpha_v\beta_3$ over-expressed targeting cyclic arginine-glycine-aspartic acid-peptide and labeled with positron radionuclide copper-64 (^{64}Cu-$MnFe_2O_4$-NPs-dopa-PEG-DOTA/RGD). *In vivo* PET/MRI of mice showed that these NPs could accurately image the tumor site with over expression of $\alpha_v\beta_3$ locally (Shi and Shen, 2018). All of these indicate Mn-NPs, particularly Mn oxide NPs, play a crucial part in PET/MRI, which is expanded for early detection and diagnosis of cancer.

5.1.3 Photoacoustic Imaging

Photoacoustic imaging (PAI) is a mixed imaging modality that merges optical illumination and ultrasound detection (Attia et al., 2019). The photothermal effect, which kills tumor cells, produces sound waves that can be detected and converted into imaging signals. This technique is capable of detecting changes of several biologically relevant signals in the TME, such as acidic pH, certain enzymes and ROS. Furthermore, PAI is useful to help the surgical removal of tumor because of its instant diagnostic functions. Photothermal transduction agents (PTAs) have a strong photothermal effect, which can harvest energy from light and convert it into heat, thereby increasing the temperature of the surrounding environment to 41~55°C and inducing tumor cells death, so PTAs can be used for PAI to build intrinsic theranostic platforms, in which imaging probes can clearly emerge the presence of tumors (Shah et al., 2008). PTAs are expected to only increase the temperature of TME locally to reduce damage to healthy tissues, where PTAs are absent or outside the range of laser irradiation.

A series of Mn oxide NPs have been widely and successfully used as PTAs due to their high absorption cross-section and strong redox property, such as Hu et al. developed a new smart nanoplatform based on degradable MnO_2-NPs (PBP@MnO_2-NPs) and a near-infrared (NIR) absorptive polymer conjugated with BODIPY molecules for dual-activatable tumor MRI/PAI. The designed smart probe had two PAI channels, in

which H_2O_2-/pH-sensitive MnO_2-NPs provide a clear PAI signal at 680 nm, and H_2O_2-/pH-inert polymer-NPs provide a bright PAI signal at 825 nm. PBP@MnO_2-NPs acted as a proportional agent with slight interference for PAI *in vivo*, and the Mn^{2+} ions released by PBP@MnO_2-NPs under TME could accurately reveal the location and size of the tumor by activated MRI (Hu et al., 2019). Beyond that, Rich et al. designed ultra-small $NaYF_4$:Nd^{3+}/$NaGdF_4$ nanocrystals coated with MnO_2 (MnO_2@ $NaYF_4$:Nd^{3+}/$NaGdF_4$-NPs) to treat head and neck squamous cell carcinomas (HNSCC), and the ability of which to increase the release of oxygen (O_2) in TME both *in vitro* and *in vivo* had been confirmed using MRI/PAI (Rich et al., 2020). Hence, these studies promise the discovery of Mn-NPs as theranostic PTAs for fast and accurate diagnosis of cancer.

5.1.4 Fluorescence Imaging

Fluorescence imaging (FI) is a common testing method in biology and medical experiments, especially broad adhibition of which in cancers. This means has superior value in accurate and early detection of tumor cells in clinical trials. Mn-NPs can selectively accumulate at the tumor site by functionalized modifications. Take advantage of this characteristic of Mn-NPs, some fluorescent dyes modifications of Mn-NPs can improve the molecular imaging of ultra-small tumor cells that cannot be detected by other imaging methods. However, the limited tissue penetration depth and autofluorescence limit its application in deep tissues (Leblond et al., 2010), thus combining MRI and FI can make up for the shortcomings of each individual pattern. MRI can provide a macroscopic boundary of the tumor for preoperative planning, while high-resolution FI can directly display the edge of the tumor during surgery, ensuring that the tumor is completely removed during surgery and normal tissue is preserved. For instance, Abbasi et al. developed polymeric theranostic NPs (PTNPs) containing a fluorescent dye (Myrj 59) and MnO-NPs for dual modal MRI/FI of breast cancer, and these NPs showed effective tumor accumulation and enhancement of MRI/FI signal in a mice xenograft orthotopic human breast tumor model (Abbasi et al., 2015). Banerjee et al. found that pyrrolidin-2-one (Pyrr)-capped Mn oxide NPs (MnO^{pyrr}-NPs) not only were qualified for Cas of MRI, but also had good photoluminescent property due to the modification of Pyrr during the thermal treatment (Banerjee et al., 2019). In the previous content, the application of SF@MnO2-NPs for MRI/FI was also reported (Yang et al., 2019). Beyond that, Mn-doped PB NPs showed excellent performance in MRI/FI of pediatric brain tumors *in vivo* (Dumont et al., 2014). We are convinced that the great potential of Mn-NPs in FI would be devoted to assist clinicians to conduct accurate and early detection of tumor cells.

5.1.5 X-Ray Imaging and X-Ray Computed Tomography Imaging

X-ray imaging is the most widely available, fastest and most cost-effective medical imaging technique today. X-ray computed tomography (CT) imaging, which is an upgraded version of X-ray imaging, has some advantages in cancer diagnosis, such as a high density and space distinguishable abilities (Pfeiffer et al., 2020). Mn-NPs have the relatively high atomic number and X-ray absorption coefficient, which makes for an X-ray contrast agent. For instance, Zhao et al. reported that Bi@mSiO_2@MnO_2/DOX-NPs could be used as excellent contrast agents for CT imaging of tumors with a high CT value (Zhao et al., 2021). Besides, Wang et al. found that multifunctional MnO_2-mSiO_2@Au-HA-NPs could simultaneously perform significant multispectral optoacoustic tomography (MSOT)/CT/MR imaging (Siyu Wang et al., 2019). Wang et al. developed MPDA-WS_2@MnO_2-NPs as trimodality contrast agents for MSOT/CT/MRI that could accomplish real-time guidance and monitoring during cancer treatment (Yidan Wang et al., 2019). It can be seen that the addition of MnO_2 into NPs will help expand their functions and enhance their applications in CT.

5.2 Therapy

The most traditional cancer therapies include chemotherapy, radiotherapy, and surgery, in which the patients may suffer from severe side effects and unsatisfied treatment outcomes. These treatment failures have inspired the development of more safe and effective treatment strategies for cancer. The emerging cancer therapies include but are not limited to photodynamic therapy (PDT), photothermal therapy (PTT), magnetic hyperthermia, immunotherapy, gene therapy (**Figure 5**), which have or may improve treatment outcomes (Liu et al., 2019a). Particularly, the simultaneous therapy of tumors by loading therapeutic drugs in Mn-NPs or combining certain clinical treatments has been widely studied and has been a hot area of current research.

5.2.1 Chemotherapy

Chemotherapy is a common treatment for cancer which makes use of chemical drugs. Traditional delivery of chemotherapeutic drugs involves oral or intravenous administration, which results in a systemic distribution of the drug, with only a small part of it reaching the tumor site. Consequently, these chemotherapeutic drugs are inevitably endocytosed by normal cells, causing serious side effects. Furthermore, chemotherapeutic drug resistance usually occurs owing to over-expression of drug efflux pumps, increased drug metabolism, and alteration of drug targets in tumor cells under constant drug stimulation. These imperfections of cancer chemotherapy are overcome by targeted drug delivery approaches, in which specific drugs or bioactive substances are released at a specific location in a controlled way (Singh et al., 2018). The fast development of nanomedicine offers great possibilities for targeted drug delivery. The ligands of tumor specific biomarkers such as monoclonal antibodies, aptamers, peptides, and vitamins all can be conjugated on to the surface of Mn-NPs containing chemotherapeutic drugs to realize targeted drug delivery. Then, these ligands interact with receptors on tumor cells, allowing endocytosis and subsequent release of the drug. Due to the small size of Mn-NPs, they can efficiently cross the capillaries to approach their target tumor cells. Mn-NPs have great biocompatibility, non-toxic nature and especially high loading capacity (Felton et al., 2014). According to these properties of Mn-NPs, they are considered as a potential drug delivery system which can be used in chemotherapy of cancer.

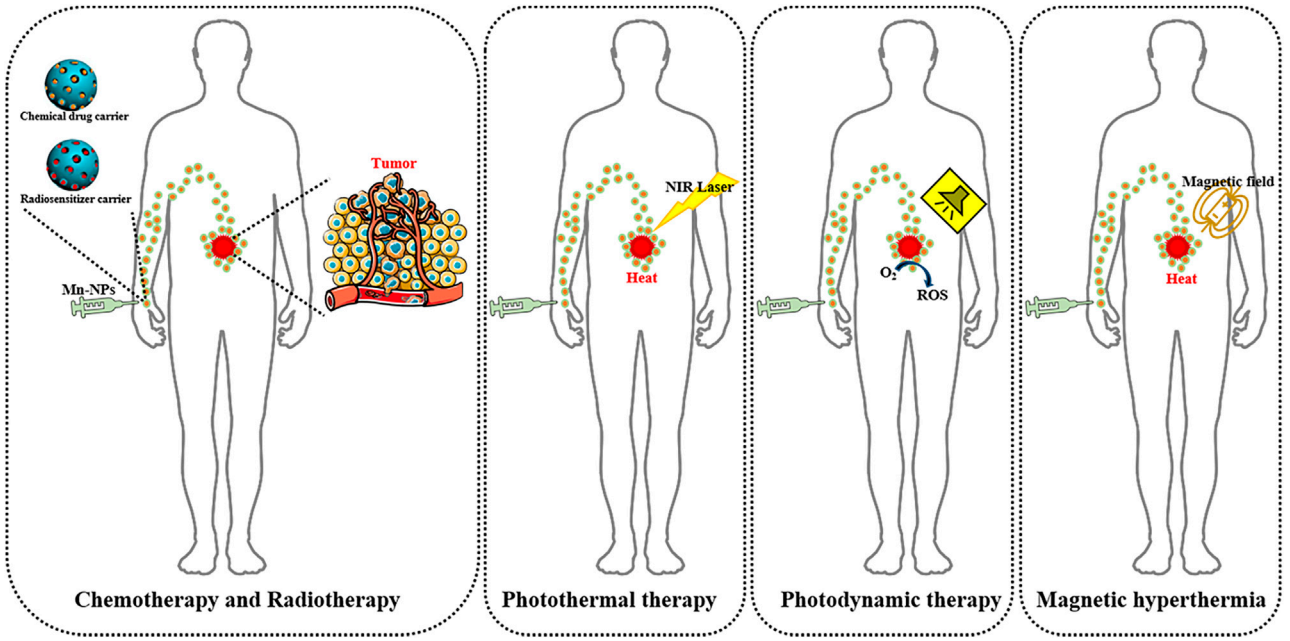

FIGURE 5 | Different approaches of Mn-NPs in cancer treatment.

Song et al. reported that high responsiveness of MnO_2-NPs to H_2O_2, which concurrently generated O_2 and regulated pH, could effectively alleviate tumor hypoxia and contribute to improve chemotherapy response in solid tumors. Additionally, hyaluronic acid (HA) modification was helpful to further enhance this ability of MnO_2-NPs. The HA-coated, mannan-conjugated MnO_2-NPs (Man-HA-MnO_2-NPs) treatment notably increased tumor oxygenation and down-regulated the expression of hypoxia-inducible factor-1α (HIF-1α) and vascular endothelial growth factor (VEGF) in breast tumor. Compared with single classical chemotherapeutic drug doxorubicin (DOX) treatment, Man-HA-MnO_2-NPs combined with DOX treatment of breast tumor observably increased the diffusion coefficient and inhibited tumor growth and tumor cell proliferation (Song et al., 2016). Yang et al. synthesized SF@MnO_2-NPs, which were co-loaded with a photodynamic agent indocyanine green (ICG) and DOX to produce a SF@MnO_2/ICG/DOX nanocomplex (SMID-NC). They demonstrated that SMID-NC could effectively accumulate in tumor-specific site via EPR effect using FI and MRI *in vivo*, and significantly improved tumor suppressive efficacy of chemotherapy with minimal systemic side effects (Yang et al., 2019).

In addition, Hou et al. reported that DOX could be enveloped in amorphous porous Mn phosphate NPs (PL/APMP-DOX). These NPs had remarkable antitumor efficacy in prolonging the lifetime of the tumor-bearing mice (Hou et al., 2020). Ren et al. described that DOX could be also packeted inside the lumen of hollow Mn/cobalt oxide NPs (MCO-DOX-NPs) and be fast released under the condition of increased glutathione (GSH) in acidic TME. MCO-DOX-NPs showed great inhibition effects in brain tumor growth both *in vitro* and *in vivo* (Ren et al., 2019). Another anticancer chemotherapeutic drug docetaxel (DTX) was co-loaded into PTNPs, and PTNPs exhibited high-efficiency drug loading, continuous and steady drug release, and higher cytotoxicity to human breast cancer cells than DTX alone *in vitro* (Abbasi et al., 2015). Moreover, Tang et al. discovered that Mn-doped silica NPs containing a special chemotherapeutic drug for liver cancer sorafenib (FaPEG-MnMSN@SFB-NPs) had efficient antitumor activity (Tang et al., 2020). These Mn-based targeted drug delivery systems provide evidence for the potential applications of Mn-NPs in cancer chemotherapy.

5.2.2 Radiotherapy

Radiotherapy (RT) is another frequently-used treatment for cancer, which depends on employing high-energy radiation to kill tumor cells. Radiosensitizers can efficiently increase the radiation dose at the cellular level, consequently improving the effect of RT. Mainstream radiosensitizers include alkylating agents that cause DNA damage, inhibitors that block DNA repair, and cell cycle synchronization agents that arrest tumor cells at the more radiosensitive G_2/M phase (Liuyun Gong et al., 2021). However, the efficient and specific delivery of these radiosensitizers, same as chemotherapeutic drugs, is also a challenge of RT. In addition, the hypoxic TME induces the radioresistance of tumors, which brings many troubles to clinicians.

Several research groups have demonstrated that inorganic NPs-based radiosensitizers are a promising choice for RT (Calugaru et al., 2015). Thereinto, Mn oxide NPs showed excellent potentials for their unique properties. They could function as not only a good radiosensitizer carrier, but also both a catalase and an oxidant that promoted decomposition of H_2O_2 into O_2 to convert the hypoxic TME, thus enhancing

RT efficacy (Siyu Wang et al., 2019). Let us cite, Meng et al. delivered the HIF-1 inhibitor acriflavine toward the tumor site to surmount hypoxia-induced radioresistance via a ROS responsive nanoplatform based on MnO_2-NPs, thus enhancing tumor oxidative repair of DNA damage and initiating O2-dependent HIF-1α degradation at the same time (Meng et al., 2018). In particular, Cho et al. discovered that MnO_2-NPs treatment had striking cytotoxic effects on non-small-cell lung cancer (NSCLC) cells and could achieve extra dose-dependent therapeutic effects (Cho et al., 2017). Besides, various functional modifications of Mn dioxide NPs contribute to optimize their aforesaid properties. Liu et al. also reported that acridine orange (AO), which can cause DNA damage under X-ray irradiation, was loaded onto MnO_2-NPs, making it a potential approach to enhance the efficacy of RT (Liu et al., 2020). Yao et al. fabricated a new kind of Bi_2Se_3-MnO_2 nanocomposites that were templated by bovine serum albumin (BSA) (Bi_2Se_3-MnO_2@BSA) via biomineralization. In this, MnO_2 as catalase could increase the O_2 concentration in TME via facilitating the decomposition of endogenous H_2O_2 in order to improve the hypoxia-induced radiation resistance of tumors (Yao et al., 2021). Tao et al. designed PEG-modified reduced nano-graphene oxide-Mn dioxide (rGO-MnO_2-PEG) nanocomposites, and used the radioisotope (^{131}I) to label these nanocomposites as radiosensitizers for *in vivo* tumor RT, ultimately obtaining significant tumor killing effects and further raising the therapeutic effects of RT (Tao et al., 2018). Shin et al. suggested that fucoidan-coated MnO_2-NPs (Fuco-MnO_2-NPs) might enhance the therapeutic effects of RT by dual targeting of tumor hypoxia and angiogenesis (Shin et al., 2018).

Meanwhile, numerous Mn-doped NPs also received elaborative studies. Bao et al. showed the whole process of a nanoscale metal-organic framework based on hafnium (Hf) cluster and Mn(III)-porphyrin ligand (fHMNM) development and production in details, and put them into use as a high-powered multifunctional theranostic agent of RT sequentially getting amazing therapeutic effect (Bao et al., 2020). Wang et al. demonstrated a nanoparticle-loaded block copolymer micellar system, based on HA-modified Mn-zinc ferrite magnetic NPs (MZF-HA-NPs), was able to be used for RT of NSCLC and played good performance in RT efficacy (Haimei Wang et al., 2020). Li et al. synthesized Au@MnS@ZnS NPs with PEG functionalization (Au@MnS@ZnS-PEG-NPs) and found that these NPs could enhance RT induced tumor cells killing efficiency (Li et al., 2016). These researches indicate that Mn-NPs have broad application prospect in the field of RT.

5.2.3 Photothermal Therapy

Photothermal therapy (PTT) is a novel cancer treatment technology that utilizes NPs to convert NIR light energy into thermal energy to ablate tumors (Zhi et al., 2020). Additionally, the PA cavitation can excite water to generate abundant ROS such as superoxide radical (O_2^-), which further spontaneously reacts with the *in situ* released NO to burst highly cytotoxic peroxynitrite ($ONOO^-$), resulting in promoting mitochondrial damage and DNA fragmentation to initiate programmed tumor cell death to treat cancer (Wang et al., 2021). This treatment technology has attracted much current attention owe to its remarkable advantages, such as non-traumatic, a short treatment time and high special spacetime control. In most cases, Mn-NPs as PTAs could be used for both PAI and PTT synchronously because of their powerful oxidizing property to establish expedient theranostic platform for monitoring and evaluating therapeutic effects. To illustrate, SMID-NC exerted a mighty and jarless photothermal effect with NIR irradiation for PTT owing to the distinct photothermal response of SF@MnO_2(Yang et al., 2019). Liu et al. prepared PEGylated amorphous MnO_2 coated polydopamine (PDA) core-shell NPs (PDA@MnO_2-PEG-NPs) with regular morphology and uniform dimensions for acid-sensitive MRI-guided tumor PTT (Liu et al., 2019b). Wen et al. showed that MnO_2-ICG@BSA had a strong singlet O_2-generation ability as well as high photothermal conversion efficiency and stability, especially possessed a significant inhibitory effect on the melanoma *in vitro* and *in vivo* (Wen et al., 2021).

PTT with the combination of other treatments is able to acquire great outcomes. Besides above, Wang et al. designed a gold with MnO_2 core-shell nanostructure (Au@MnO_2) as a GSH-triggered intelligent theranostic agent for dual-MRI/PAI-guided chemodynamic therapy (CDT) and PTT, and confirmed their excellent synergistic treatment effects in CDT/PTT (Yijue Wang et al., 2020). Soratijahromi et al. synthesized a gold with MnO_2 nanocomposite (Au/MnO_2-NC) as a new type photo- and sono-responsive nanomedicine that worked upon laser irradiation or ultrasound exposure for applications in PTT and sonodynamic therapy (SDT) of cancer (Soratijahromi et al., 2020). In addition, some Mn-doped NPs also had broad application prospects in PTT, such as Wu et al. discovered that magnetic-luminescent folic acid-conjugated NPs ($MnFe_2O_4$-$NaYF_4$ Janus-NPs) had a high cellular uptake efficiency in human esophageal carcinoma cells (Eca-109 cells) own to their upconversion luminescence properties and folate targeting potential. These NPs could strongly absorb light in the NIR range and fast convert to thermal energy, in order to remarkedly kill Eca-109 cells upon 808 nm laser irradiation. Furthermore, the growth of Eca-109 cells tumors in mice was availably restrained by the photothermal effects of $MnFe_2O_4$-$NaYF_4$ Janus-NPs(Wu et al., 2017). Zhang et al. developed a therapeutic nanoplatform based on Mn-doped iron oxide NPs that were modified denatured BSA (MnIO-dBSA-NPs). *In vitro* experiments showed great photothermal effects of MnIO-dBSA-NPs, and *in vivo* experiments further proved that these NPs could effectively ablate the tumor tissue achieved light irradiation (Zhang et al., 2015). Yang et al. also reported that graphene oxide (GO)/$MnFe_2O_4$-NPs had strong light absorption capacity and good photothermal stability in NIR region, and could give rise to the worthy photothermal ablation of cancer cells (Yang et al., 2016). These studies showed that Mn-NPs possessed enormous potential and application values in PTT of cancer.

5.2.4 Photodynamic Therapy

Photodynamic therapy (PDT) is a clinically approved cancer therapy that uses non-toxic dyes and harmless visible light in combination with O_2 to produce high level of ROS to kill tumor

cells (Castano et al., 2006). As we all known, the hypoxic TME is a challenge for cancer treatments. The obtained product of Mn oxide NPs could reactive with endogenous H_2O_2 in TME strongly, which was decomposed into O_2 to improve PDT of cancer (Yang et al., 2019). Liu et al. prepared the hybridized nanoplatform (R-MnO_2-FBP) by assembly of Rhodamine B (RhB)-encapsulated MnO_2 as O_2 supplier and indicator, and fluorescein isothiocyanate (FITC)-labelled peptide-functionalized black phosphorus as the theranostic agent. After specific delivery towards tumor cells, R-MnO_2-FBP decomposed in the acidic and H_2O_2-rich TME and produced O_2 to confront hypoxia-induced PDT resistance, in which released Mn^{2+} and RhB dye to realize dual-mode MRI/FI monitoring of O_2 self-supply process. Importantly, imaging-guided PDT using R-MnO_2-FBP showed 51.6% of apoptosis in hypoxic cells (Liu et al., 2019c). Yin et al. developed a H_2O_2-responsive nanozyme (AuNCs@mSiO_2@MnO_2) for off/on modulation and enhancement of MRI-guided PDT, in which MnO_2 nanosheets were wrapped as switch shielding shell. In a neutral physiological environment, the stable MnO_2 shell could eliminate the production of singlet O_2, thereby turning off MRI and PDT. Nevertheless, the reaction of MnO_2 shell with H_2O_2 could induce the degradation of MnO_2 to turn on MRI and PDT in the acidic TME, and the generated O_2 further enhanced PDT (Yin et al., 2021). Liang et al. developed the core-shell gold nanocage with MnO_2 NPs (AuNC@MnO_2-NPs) as TME responsive O_2 generators and NIR-triggered ROS producers for O_2-boosted immunogenic PDT against metastatic triple-negative breast cancer (Liang et al., 2018).

Similarly, PDT combined with other treatment methods can achieve better curative effect. The combination of PDT and enzyme therapy is a very suitable treatment for tumors because it exploits the dimensional control of PDT and efficient enzyme-catalyzed biological reactions. However, co-encapsulation of hydrophilic enzymes and hydrophobic photosensitizers is a challenge, because these two agents often interfere with each other. The development of Mn-doped NPs is expected to solve this problem. For example, Zhu et al. developed a protocell-like nanoreactor, in which hydrophilic glucose oxidase (GOx) was loaded in the pores of mesoporous silica NPs, and hydrophobic Mn phthalate (MnPc) was loaded in the membrane layer of liposomes middle, for synergistic starvation therapy and PDT. The spatial separation of these two payloads protected GOx and MnPc from the cellular environment and avoided mutual influence. GOx catalyzed the oxidation of glucose to generate H_2O_2 and gluconic acid, causing cancer cells to undergo starvation therapy by consuming glucose while disrupting cellular redox balance. MnPc could generate cytotoxic singlet O_2 under 730 nm laser irradiation to conduct PDT. A single treatment of GOx-MSN@MnPc-LP could effectively inhibit tumor growth, indicating a strong synergistic effect of starvation therapy and PDT, which was validated *in vitro* and vivo experiments (Zhu et al., 2020). Additionally, Irmania et al. synthesized Mn-doped green tea-derived carbon quantum dots (Mn-CQDs) as a targeted dual imaging and PDT nanoplatform, and *in vitro* cell viability studies verified Mn-CQDs upon 671 nm irradiation were able to kill more than 90% of tumor cells in PDT (Irmania et al., 2020). Atif et al. reported that Mn-doped cerium nanocomposites enhanced the antibacterial activity and effectiveness of PDT, which might be related to the maximal ROS generation from targeted toxicity and maximal antioxidant activity in bacterial growth inhibition (Atif et al., 2019). As can be seen, Mn-NPs might provide additional benefits to enhance PDT.

5.2.5 Magnetic Hyperthermia

Magnetic hyperthermia is a treatment technique that raises the temperature of a specific tissue above 46°C, which is pretty above the normal physiological temperature (36~37°C), to kill tumor cells under the controlled magnetic field (Farzin et al., 2020). Cancerous cells are more sensitized to hyperthermia compared to normal cells, due to the reducation of the pH at TME causing decreased thermotolerance. The implement of magnetic hyperthermia is inseparable from the use of magnetic NPs (MNPs) (Iacovita et al., 2019). Magnetite (Fe_3O_4) and maghemite (γ-F_2O_3) are the only category of MNPs approved for clinical use by the US Food and Drug Administration (Wilczewska et al., 2012). However, iron oxide MNPs have limited value in magnetic moments, causing the restrictive heating capacity. To figure out these difficulties, new kinds of MNPs have been persistently developed, aimed to obtain better magnetic properties.

Mn becomes a good option for this improvement approach of MNPs owing to its outstanding biocompatibility. For instances, Haghniaz et al. firstly reported that the dextran-coated lanthanum strontium MnO_3-NPs (Dex-LSMO-NPs) had strong ferromagnetism and low Curie temperature and were suitable for hyperthermia applications *in vivo* (Haghniaz et al., 2016). Other than that, CS-coated $MnFe_2O_4$ NPs also showed great magnetic properties, especially used in hyperthermia studies for biomedical research (Islam et al., 2020). MZF-HA-NPs were developed for synergistic therapy under alternating magnetic field and radiation field (Haimei Wang et al., 2020). We believe that MNPs will obtain better effectiveness and wider applications in diagnosis and treatment of cancer, with the further research in Mn coating.

5.2.7 Immunotherapy

Cancer immunotherapy has drawn much attention and achieved continued advancements especially for its safety and amazing prognosis (Yang et al., 2021). Yang et al. developed an intelligent biodegradable hollow Mn dioxide (H-MnO_2) nanoplatform that served for on-demand drug release and modulation of hypoxic TME to enhance cancer immunotherapy. H-MnO_2 nanoshells post modification with polyethylene glycol (PEG) were co-loaded with a photodynamic agent chlorine e6 (Ce6) and DOX (H-MnO_2-PEG/C&D-NPs). As a result, an arresting *in vivo* synergistic therapeutic effect was gained via the combined chemo-PDT, which also triggered a series of anti-tumor immune responses at the same time (Yang et al., 2017). Cyclic GMP-AMP synthase (cGAS) and stimulator of interferon genes (STING) are vital components of the innate immune sensors to cytosolic DNA. Mn was reported to comprehensively induce the activation of cGAS and STING from heightening cGAMP

TABLE 1 | Summary of the application of Mn-NPs in cancer diagnosis and therapy.

NPs	Size	Applications	Cell lines	Animal model	Ref
SMID-NC	60 nm	MRI, FI, chemotherapy, PTT, PDT	4T1 cells	Balb/c 4T1 tumor-bearing mice	Yang et al. (2019)
Gd-MnMEIO-NPs	12 nm	MRI	CT26 cells	Balb/c CT26 xenograft liver tumor mice	Kuo et al. (2016)
MnPB-NPs	33 nm	MRI, FI	brainstem glioma (BSG) D10 cells	Balb/c BSG D10 tumor-bearing mice	Dumont et al. (2014)
^{64}Cu-NOTA-Mn_3O_4@PEG-TRC105-NPs	7 nm	MRI, PET	4T1 cells, HEK-293 cells, HUH-7 cells, MCF-7 human breast cancer cells, human umbilical vein endothelial cells	Balb/c 4T1 tumor-bearing mice	Zhan et al. (2017)
^{64}Cu-NOTA-FA-FI-PEG-PEI-Ac-Mn_3O_4-NPs	7.29 nm	MRI, PET	HeLa cells	Nude HeLa tumor-bearing mice	Zhu et al. (2018)
^{64}Cu-$MnFe_2O_4$-NPs-dopa-PEG-DOTA/RGD	5 nm	MRI, PET	U87MG cells	Nude U87MG tumor-bearing mice	Shi and Shen, (2018)
PBP@MnO2-NPs	93 nm	MRI, PAI	4T1 cells	Xenograft 4T1 tumor mice	Hu et al. (2019)
MnO_2@ $NaYF_4$:Nd^{3+}/$NaGdF_4$-NPs	4.13 nm	MRI, PAI	None	SCID mice bearing tumor from a HNSCC patient-derived xenograft	Rich et al. (2020)
PTNPs	13 nm	MRI, FI, chemotherapy	MDAMB-231 cells	SCID breast tumor-bearing mice	Abbasi et al. (2015)
MnO^{pyrr}-NPs	8.1 nm	MRI, FI	HeLa cells, HepG2 cells	None	Banerjee et al. (2019)
Bi@$mSiO_2$@MnO_2/DOX-NPs	30 nm	MRI, CT, chemotherapy, PTT, CDT	human umbilical vein endothelial cells, HeLa cells	Nude HeLa tumor-bearing mice	Zhao et al. (2021)
MnO_2-$mSiO_2$@Au-HA-NPs	196.9 nm	MRI, CT, MSOT, RT, PTT	4T1 cells	Nude 4T1 tumor-bearing mice	Siyu Wang et al. (2019)
MPDA-WS_2@MnO_2-NPs	170 nm	MRI, CT, MSOT, RT	4T1 cells	Nude 4T1 tumor-bearing mice	Yidan Wang et al. (2019)
Man-HA-MnO_2-NPs	203 nm	Chemotherapy	4T1 cells	Balb/c 4T1 tumor-bearing mice	Song et al. (2016)
PL/APMP-DOX	3.88 nm	Chemotherapy	4T1 cells	Balb/c 4T1 tumor-bearing mice	Hou et al. (2020)
MCO-DOX-NPs	70 nm	MRI, chemotherapy	U87MG cells	Nude U87MG tumor-bearing mice	Ren et al. (2019)
FaPEG-MnMSN@SFB-NPs	101 nm	Chemotherapy	HepG2 cells	Nude HepG2 tumor-bearing mice	Tang et al. (2020)
MnO_2-NPs	30 nm	RT	CT26 cells, 4T1 cells	CT26 tumor-bearing mice, 4T1 tumor-bearing mice	Meng et al. (2018)
MnO_2-NPs	49.81 nm	RT	NSCLC cells	None	Cho et al. (2017)
MnO_2-NPs	155.5 nm	RT	H1299 cells	Nude H1299 xenograft tumor mice	Liu et al. (2020)
Bi_2Se_3-MnO_2@BSA	38 nm	RT	4T1 cells	Balb/c 4T1 tumor-bearing mice	Yao et al. (2021)
rGO-MnO_2-PEG	24 nm	RT	4T1 cells	Balb/c 4T1 tumor-bearing mice	Tao et al. (2018)
Fuco-MnO_2-NPs	17 nm	RT	human pancreatic cancer cell lines (AsPC-1 and BxPC-3)	Balb/c nude mice bearing BxPC3 xenograft tumors	Shin et al. (2018)
fHMNM	4 nm	MRI, PAI, CT, RT, PTT	Hela cells, 4T1 cells, MCF10A cells and S180 cells	Balb/c S180 tumor-bearing mice	Bao et al. (2020)
MZF-HA-NPs	150 nm	RT, magnetic hyperthermia	A549 cells, Beas-2B cells	Balb/c nude A549 tumor-bearing mice	Haimei Wang et al. (2020)
Au@MnS@ZnS-PEG-NPs	110 nm	MRI, RT	4T1 cells	Balb/c 4T1 tumor-bearing mice	Li et al. (2016)
PDA@MnO_2-PEG-NPs	120 nm	MRI, PTT	4T1 cells	Balb/c 4T1 tumor-bearing mice	Liu et al. (2019b)
MnO_2-ICG@BSA	44.67 nm	PTT, PDT	B16F10 cells	Nude B16F10 tumor-bearing mice	Wen et al. (2021)
Au@MnO_2	25 nm	MRI, PAI, PTT, CDT	4T1 cells	Balb/c 4T1 tumor-bearing mice	Yijue Wang et al. (2020)
Au/MnO_2-NC	2 μm	PTT, sonodynamic therapy	Mouse threatening melanoma cell line C540 (B16/F10)	Balb/c C540 tumor-bearing mice	Soratijahromi et al. (2020)
$MnFe_2O_4$-$NaYF_4$ Janus-NPs	13.1 nm	PTT	QSG-7701 cells, Eca-109 cells	Balb/c Eca-109 tumor-bearing mice	Wu et al. (2017)
MnIO-dBSA-NPs	5 nm	MRI, PTT	4T1 cells	Balb/c 4T1 tumor-bearing mice	Zhang et al. (2015)
GO/$MnFe_2O_4$-NPs	170 nm	MRI, chemotherapy, PTT	HeLa cells, L929 cells	Nude HeLa tumor-bearing mice	Yang et al. (2016)
R-MnO_2-FBP	120 nm	MRI, FI, PDT	HeLa cells	Nude HeLa tumor-bearing mice	Liu et al. (2019c)
AuNCs@$mSiO_2$@MnO_2	140 nm	MRI, PDT	MDA-MB-435 cells	Nude MDA-MB-435 tumor-bearing mice	Yin et al. (2021)

(Continued on following page)

TABLE 1 | (*Continued*) Summary of the application of Mn-NPs in cancer diagnosis and therapy.

NPs	Size	Applications	Cell lines	Animal model	Ref
AuNC@MnO_2-NPs	91 nm	MRI, PAI, FI, PDT	4T1 cells	Balb/c 4T1 tumor-bearing mice	Liang et al. (2018)
GOx-MSN@MnPc-LP	177 nm	PDT	4T1 cells	Balb/c 4T1 tumor-bearing mice	Zhu et al. (2020)
Mn-CQDs	5 nm	MRI, FI, PDT	HeLa cells	Nude HeLa tumor-bearing mice	Irmania et al. (2020)
Mn-doped ceria nanocomposite	27.2 nm	PDT	MCF-7 cells	None	Atif et al. (2019)
Dex-LSMO-NPs	25–50 nm	magnetic hyperthermia	B16F1 cells	C57BL/6J B16F1 tumor-bearing mice	Haghniaz et al. (2016)
H-MnO_2-PEG/C&D-NPs	3.94 nm	Chemotherapy, PDT, immunotherapy	4T1 cells	Balb/c 4T1 tumor-bearing mice	Yang et al. (2017)
DCMNs	78 nm	Chemotherapy, PDT, immunotherapy	HeLa cells, 4T1 cells	Balb/c 4T1 tumor-bearing mice	Geng et al. (2021)
Mn@CaCO3/ICG-NPs	107.5 nm	PDT, gene therapy	Lewis lung tumor cells	Balb/c Lewis lung tumor-bearing mice	Liu et al. (2019d)
HART nanoassembly	314 nm	MRI, chemotherapy, gene therapy	MCF7/ADR cells	None	Rajendrakumar et al. (2019)
MnO_2 nanosheets	6 nm	Chemotherapy, gene therapy	A549 cells, MDA-MB-231 cells	Nude MDA-MB-231 xenograft tumor mice	Nie et al. (2020)

production to strengthening cGAMP/STING binding affinity (Wang et al., 2018). Thus, DOX was enveloped in APMP-NPs to gain better synergetic antitumor effects through the activation of cGAS/STING pathway (Hou et al., 2020). A battery of antibodies targeting cellular immune checkpoints, such as PD-1/PD-L1 and CTLA-4, have been developed to promote the activation of T cells and succedent tumor treatment (Van Allen et al., 2015; McGranahan et al., 2016; Le et al., 2017). The rapid development of Mn-NPs is helpful for making use of these antibodies. Geng et al. synthesized Ce6 and DOX coating Mn-NPs (DCMNs) to increase antitumor responses of PD-1 via the combination of chemotherapy and PDT (Geng et al., 2021). The properties of Mn-NPs can greatly improve the efficacy of immunotherapy.

5.2.6 Gene Therapy

Gene therapy was first used genetic material to treat inherited diseases, but it was soon used in cancer treatment (Husain et al., 2015). One of the most important advances in gene therapy of cancer is the application of small interfering RNA (siRNA), which is able to regulate the expression of genes by RNA interference (RNAi). However, despite the potential and powerful functions of these molecules, several shortcomings make their clinical application difficult, including delivery problems, off-target effects, interference with physiological functions of cellular mechanisms involved in gene silencing, and induction of innate immune responses. The appearance of NPs systems provides an ideal opportunity to conquer these troubles (Miele et al., 2012; Zaimy et al., 2017).

Mn-NPs are an excellent gene delivery system which is able to efficiently package siRNA, avoiding its degradation along with serious immune response in the organisms (Bae et al., 2011). Liu et al. synthesized Mn@CaCO3/ICG-NPs loaded with PD-L1-targeting siRNA to enhance the effect of PDT while inhibiting tumor cell resistance/escape with the combination of PDT and immunotherapy. *In vivo* experiments showed that Mn@CaCO3/ICG-NPs could effectively deliver drugs to tumor tissues, significantly redress tumor hypoxia, and further enhance the therapeutic effect of PDT. Besides, the synergistic benefit of siRNA silenced PD-L1 gene that mediated immune resistance/evasion, bringing an amazing therapeutic effect by rousing the immune system (Liu et al., 2019d). Rajendrakumar et al. packaged DOX and antiapoptotic protein B-cell lymphma 2 (Bcl-2) shRNA encoded plasmid into Mn_3O_4 and Fe_3O_4 NPs (HART nanoassembly) with a green-synthesized method. The synergistic cytotoxic effect of Bcl-2 silencing and DOX was acquired by successfully transfecting these NPs into MCF7 multidrug-resistant breast cancer cells (Rajendrakumar et al., 2019).

The RNA-cleaving DNA zyme (DZ) has better prospects for RNAi applications than siRNA because of its higher chemical stability, biocompatibility, predictable activity, and substrate versatility. However, its pharmaceutical applications for disease treatment are confined by the need of metal cofactor for activation and the lack of reliable co-delivery systems in combination with other therapeutic manners. Nie et al. developed metal organic framework coated MnO_2 nanosheets to realize the co-delivery of a survivin inhibiting DZ and DOX for combined chemo-gene therapy in cancer (Nie et al., 2020). Thereout, Mn-NPs provide a good model for designing efficient, customizable nanocarriers for gene therapy of cancer.

Table 1 summarized the application of Mn-NPs in cancer diagnosis and therapy in details.

6 FUTURE PERSPECTIVE AND CHALLENGES

As we all known, cancer is a multi-system disease caused by numerous factors. Therefore, the combination of diagnosis and therapy modalities is significantly necessary for anti-cancer work. The use of multifunctional therapeutic agents in multimodal imaging and therapy is a promising strategy to overcome the limitations of single modality diagnosis and therapy, which can

effectively improve the accuracy of diagnosis and prognosis after treatment in affected cancer patients. As mentioned above, many multifunctional Mn-NPs were developed to realize the early imaging and dual even more trimodality therapy of cancer simultaneously (Xi et al., 2017; Siyu Wang et al., 2019; Yang et al., 2019).

The hypoxic TME as a major mechanism of resistance to tumor treatment may be the most severe difficulty in cancer therapy, which results in insignificant therapeutic effects and poor patient survivals (Siemer et al., 2020), and is urgent for researchers and clinicians to overcome it. Interestingly, Mn-NPs can exert anti-tumor effects through not only as a drug delivery system but also as an oxygenation agent according to past researches. When Mn-NPs are specifically distributed in tumor sites, the decomposition reaction of Mn-NPs promotes H_2O_2 into oxygen molecules, which can relieve tumor hypoxia (Meng et al., 2018). Moreover, Mn-NPs induced that disruption of redox balance would lead to apoptosis and ROS-dependent ferroptosis of tumor cells (Tang et al., 2020). Ferroptosis is a newly discovered form of cell death, which is different from apoptosis, autophagy and pyroptosis, and has unique morphological and biological metabolic changes in cells. Its mechanism is mainly characterized by the production of iron-dependent ROS: When too much ROS is produced and its antioxidant capacity is insufficient to fight it, ROS production and clearance are out of balance, leading to ferroptosis. In recent years, ferroptosis has become a research hotspot in the field of oncology (Liang et al., 2019). With the continuous attempts and applications of Mn-NPs in clinical practice, more and more studies believe that inducing the ferroptosis of tumor cells may become an effective tumor treatment.

Although the current researches on Mn-NPs for biomedical applications in cancer diagnosis and therapy have made great progress, there are still some problems that need to be alerted. Firstly, the large size of Mn-NPs has difficulty excreting from the kidney and causes accumulation in the visceral organ. Secondly, the nerve damage caused by Mn-NPs is not properly addressed. These two issues are still the biggest barriers to the inability of Mn-NPs to be used in the clinic. Thirdly, the diversity of cancer types and progression as well as the differences between affected cancer patients are hard for researchers and clinicians to make the right choice for functional modification of Mn-NPs, which require abundant efforts to resolve. Fortunately, numerous advanced computer simulation techniques can now predict the target and affinity of well-designed NPs, which can greatly reduce our workload for modifier selection of NPs including Mn-NPs. Considered the success of Mn-NPs for biological imaging and cancer treatment, we believe that Mn-NPs offer unique opportunities to translate the insights of basic research into clinical applications.

AUTHOR CONTRIBUTIONS

DN and YZ drafted the original manuscript; TG and MY contributed to writing the review; ML conceived and edited the manuscript, and was responsible for the overall direction of the paper.

FUNDING

This work was supported by the National Natural Science Foundation of China (81571797), the Social Development Plan of Taizhou, China (TS202004), the Natural Science Foundation of Nanjing University of Chinese Medicine China (XZR2020093), and Taizhou People's Hospital Medical Innovation Team Foundation, China (CXTDA201901).

ACKNOWLEDGMENTS

Special thanks to my fiancee Han Zhang, you gave me the enthusiasm for life and study. I sincerely hope to marry you soon and spend the rest of my life with you happily.

REFERENCES

Abbasi, A. Z., Prasad, P., Cai, P., He, C., Foltz, W. D., Amini, M. A., et al. (2015). Manganese Oxide and Docetaxel Co-loaded Fluorescent Polymer Nanoparticles for Dual Modal Imaging and Chemotherapy of Breast Cancer. *J. Controlled Release* 209, 186–196. doi:10.1016/j.jconrel.2015.04.020

Abulizi, A., Yang, G. H., Okitsu, K., and Zhu, J.-J. (2014). Synthesis of MnO2 Nanoparticles from Sonochemical Reduction of MnO4– in Water under Different pH Conditions. *Ultrason. Sonochem.* 21 (5), 1629–1634. doi:10.1016/j.ultsonch.2014.03.030

Ahmed, S., Annu, fnm., Chaudhry, S. A., and Ikram, S. (2017). A Review on Biogenic Synthesis of ZnO Nanoparticles Using Plant Extracts and Microbes: A prospect towards green Chemistry. *J. Photochem. Photobiol. B: Biol.* 166, 272–284. doi:10.1016/j.jphotobiol.2016.12.011

Al-Fahdawi, M. Q., Rasedee, A., Al-Qubaisi, M. S., Alhassan, F. H., Rosli, R., El Zowalaty, M. E., et al. (2015). Cytotoxicity and Physicochemical Characterization of Iron-Manganese-Doped Sulfated Zirconia Nanoparticles. *Int. J. Nanomedicine* 10, 5739–5750. doi:10.2147/IJN.S82586

Ali, L. M. A., Mathlouthi, E., Kajdan, M., Daurat, M., Long, J., Sidi-Boulenouar, R., et al. (2018). Multifunctional Manganese-Doped Prussian Blue Nanoparticles for Two-Photon Photothermal Therapy and Magnetic Resonance Imaging. *Photodiagnosis Photodynamic Ther.* 22, 65–69. doi:10.1016/j.pdpdt.2018.02.015

An, J., Hu, Y.-G., Cheng, K., Li, C., Hou, X.-L., Wang, G.-L., et al. (2020). ROS-augmented and Tumor-Microenvironment Responsive Biodegradable Nanoplatform for Enhancing Chemo-Sonodynamic Therapy. *Biomaterials* 234, 119761. doi:10.1016/j.biomaterials.2020.119761

Anderson, N. M., and Simon, M. C. (2020). The Tumor Microenvironment. *Curr. Biol.* 30 (16), R921–r925. doi:10.1016/j.cub.2020.06.081

Atif, M., Iqbal, S., Fakhar-E-Alam, M., Ismail, M., Mansoor, Q., Mughal, L., et al. (2019). Manganese-Doped Cerium Oxide Nanocomposite Induced Photodynamic Therapy in MCF-7 Cancer Cells and Antibacterial Activity. *Biomed. Res. Int.* 2019, 7156828. doi:10.1155/2019/7156828

Attia, A. B. E., Balasundaram, G., Moothanchery, M., Dinish, U. S., Bi, R., Ntziachristos, V., et al. (2019). A Review of Clinical Photoacoustic Imaging: Current and Future Trends. *Photoacoustics* 16, 100144. doi:10.1016/j.pacs.2019.100144

Bae, K. H., Lee, K., Kim, C., and Park, T. G. (2011). Surface Functionalized Hollow Manganese Oxide Nanoparticles for Cancer Targeted siRNA Delivery and

Magnetic Resonance Imaging. *Biomaterials* 32 (1), 176–184. doi:10.1016/j.biomaterials.2010.09.039

Baetke, S. C., Lammers, T., and Kiessling, F. (2015). Applications of Nanoparticles for Diagnosis and Therapy of Cancer. *Br. J. Radiol.* 88 (1054), 20150207. doi:10.1259/bjr.20150207

Banerjee, A., Bertolesi, G. E., Ling, C.-C., Blasiak, B., Purchase, A., Calderon, O., et al. (2019). Bifunctional Pyrrolidin-2-One Terminated Manganese Oxide Nanoparticles for Combined Magnetic Resonance and Fluorescence Imaging. *ACS Appl. Mater. Inter.* 11 (14), 13069–13078. doi:10.1021/acsami.8b21762

Bao, J., Zu, X., Wang, X., Li, J., Fan, D., Shi, Y., et al. (2020). Multifunctional Hf/Mn-TCPP Metal-Organic Framework Nanoparticles for Triple-Modality Imaging-Guided PTT/RT Synergistic Cancer Therapy. *Int. J. Nanomedicine* 15, 7687–7702. doi:10.2147/ijn.s267321

Bellusci, M., La Barbera, A., Padella, F., Mancuso, M., Pasquo, A., Grollino, M. G., et al. (2014). Biodistribution and Acute Toxicity of a Nanofluid Containing Manganese Iron Oxide Nanoparticles Produced by a Mechanochemical Process. *Int. J. Nanomedicine* 9, 1919–1929. doi:10.2147/IJN.S56394

Cai, X., Zhu, Q., Zeng, Y., Zeng, Q., Chen, X., and Zhan, Y. (2019). Manganese Oxide Nanoparticles as MRI Contrast Agents in Tumor Multimodal Imaging and Therapy. *Int. J. Nanomedicine* 14, 8321–8344. doi:10.2147/ijn.s218085

Calugaru, V., Magné, N., Hérault, J., Bonvalot, S., Le Tourneau, C., and Thariat, J. (2015). Nanoparticules et radiothérapie. *Bull. du Cancer* 102 (1), 83–91. doi:10.1016/j.bulcan.2014.10.002

Castano, A. P., Mroz, P., and Hamblin, M. R. (2006). Photodynamic Therapy and Anti-tumour Immunity. *Nat. Rev. Cancer* 6 (7), 535–545. doi:10.1038/nrc1894

Cho, M. H., Choi, E.-S., Kim, S., Goh, S.-H., and Choi, Y. (2017). Redox-Responsive Manganese Dioxide Nanoparticles for Enhanced MR Imaging and Radiotherapy of Lung Cancer. *Front. Chem.* 5, 109. doi:10.3389/fchem.2017.00109

Dacarro, G., Taglietti, A., and Pallavicini, P. (2018). Prussian Blue Nanoparticles as a Versatile Photothermal Tool. *Molecules* 23 (6), 1414. doi:10.3390/molecules23061414

Dumont, M. F., Yadavilli, S., Sze, R. W., Nazarian, J., and Fernandes, R. (2014). Manganese-containing Prussian Blue Nanoparticles for Imaging of Pediatric Brain Tumors. *Int. J. Nanomedicine* 9, 2581–2595. doi:10.2147/IJN.S63472

Fan, M., Han, Y., Gao, S., Yan, H., Cao, L., Li, Z., et al. (2020). Ultrasmall Gold Nanoparticles in Cancer Diagnosis and Therapy. *Theranostics* 10 (11), 4944–4957. doi:10.7150/thno.42471

Farzin, A., Etesami, S. A., Quint, J., Memic, A., and Tamayol, A. (2020). Magnetic Nanoparticles in Cancer Therapy and Diagnosis. *Adv. Healthc. Mater.* 9 (9), e1901058. doi:10.1002/adhm.201901058

Felton, C., Karmakar, A., Gartia, Y., Ramidi, P., Biris, A. S., and Ghosh, A. (2014). Magnetic Nanoparticles as Contrast Agents in Biomedical Imaging: Recent Advances in Iron- and Manganese-Based Magnetic Nanoparticles. *Drug Metab. Rev.* 46 (2), 142–154. doi:10.3109/03602532.2013.876429

Gao, X., Wang, Q., Cheng, C., Lin, S., Lin, T., Liu, C., et al. (2020). The Application of Prussian Blue Nanoparticles in Tumor Diagnosis and Treatment. *Sensors (Basel)* 20 (23), 6905. doi:10.3390/s20236905

Geng, Z., Chen, F., Wang, X., Wang, L., Pang, Y., and Liu, J. (2021). Combining Anti-PD-1 Antibodies with Mn2+-Drug Coordinated Multifunctional Nanoparticles for Enhanced Cancer Therapy. *Biomaterials* 275, 120897. doi:10.1016/j.biomaterials.2021.120897

Haghniaz, R., Umrani, R. D., and Paknikar, K. M. (2016). Hyperthermia Mediated by Dextran-Coated La0.7Sr0.3MnO3 Nanoparticles: *In Vivo* Studies. *Int. J. Nanomedicine* 11, 1779–1791. doi:10.2147/IJN.S104617

Haque, S., Tripathy, S., and Patra, C. R. (2021). Manganese-based Advanced Nanoparticles for Biomedical Applications: Future Opportunity and Challenges. *Nanoscale* 13 (39), 16405–16426. doi:10.1039/d1nr04964j

Haimei Wang, H., An, L., Tao, C., Ling, Z., Lin, J., Tian, Q., et al. (2020). A Smart Theranostic Platform for Photoacoustic and Magnetic Resonance Dual-Imaging-Guided Photothermal-Enhanced Chemodynamic Therapy. *Nanoscale* 12 (8), 5139–5150. doi:10.1039/c9nr10039c

Hoseinpour, V., and Ghaemi, N. (2018). Green Synthesis of Manganese Nanoparticles: Applications and Future Perspective-A Review. *J. Photochem. Photobiol. B: Biol.* 189, 234–243. doi:10.1016/j.jphotobiol.2018.10.022

Hou, L., Tian, C., Yan, Y., Zhang, L., Zhang, H., and Zhang, Z. (2020). Manganese-Based Nanoactivator Optimizes Cancer Immunotherapy via Enhancing Innate Immunity. *ACS Nano* 14 (4), 3927–3940. doi:10.1021/acsnano.9b06111

Hu, X., Liu, G., Li, Y., Wang, X., and Liu, S. (2015). Cell-penetrating Hyperbranched Polyprodrug Amphiphiles for Synergistic Reductive Milieu-Triggered Drug Release and Enhanced Magnetic Resonance Signals. *J. Am. Chem. Soc.* 137 (1), 362–368. doi:10.1021/ja5105848

Hu, X., Zhan, C., Tang, Y., Lu, F., Li, Y., Pei, F., et al. (2019). Intelligent Polymer-MnO2 Nanoparticles for Dual-Activatable Photoacoustic and Magnetic Resonance Bimodal Imaging in Living Mice. *Chem. Commun.* 55 (43), 6006–6009. doi:10.1039/c9cc02148e

Husain, S. R., Han, J., Au, P., Shannon, K., and Puri, R. K. (2015). Gene Therapy for Cancer: Regulatory Considerations for Approval. *Cancer Gene Ther.* 22 (12), 554–563. doi:10.1038/cgt.2015.58

Iacovita, C., Florea, A., Scorus, L., Pall, E., Dudric, R., Moldovan, A. I., et al. (2019). Hyperthermia, Cytotoxicity, and Cellular Uptake Properties of Manganese and Zinc Ferrite Magnetic Nanoparticles Synthesized by a Polyol-Mediated Process. *Nanomaterials (Basel)* 9 (10), 1489. doi:10.3390/nano9101489

Irmania, N., Dehvari, K., Gedda, G., Tseng, P. J., and Chang, J. Y. (2020). Manganese-doped green tea-derived Carbon Quantum Dots as a Targeted Dual Imaging and Photodynamic Therapy Platform. *J. Biomed. Mater. Res.* 108 (4), 1616–1625. doi:10.1002/jbm.b.34508

Islam, K., Haque, M., Kumar, A., Hoq, A., Hyder, F., and Hoque, S. M. (2020). Manganese Ferrite Nanoparticles (MnFe2O4): Size Dependence for Hyperthermia and Negative/Positive Contrast Enhancement in MRI. *Nanomaterials* 10 (11), 2297. doi:10.3390/nano10112297

Kim, B. Y. S., Rutka, J. T., and Chan, W. C. W. (2010). Nanomedicine. *N. Engl. J. Med.* 363 (25), 2434–2443. doi:10.1056/nejmra0912273

Kuo, Y.-T., Chen, C.-Y., Liu, G.-C., and Wang, Y.-M. (2016). Development of Bifunctional Gadolinium-Labeled Superparamagnetic Nanoparticles (Gd-MnMEIO) for *In Vivo* MR Imaging of the Liver in an Animal Model. *PloS one* 11 (2), e0148695. doi:10.1371/journal.pone.0148695

Law, S., Leung, A. W., and Xu, C. (2020). Folic Acid-Modified Celastrol Nanoparticles: Synthesis, Characterization, Anticancer Activity in 2D and 3D Breast Cancer Models. *Artif. Cell Nanomedicine, Biotechnol.* 48 (1), 542–559. doi:10.1080/21691401.2020.1725025

Le, D. T., Durham, J. N., Smith, K. N., Wang, H., Bartlett, B. R., Aulakh, L. K., et al. (2017). Mismatch Repair Deficiency Predicts Response of Solid Tumors to PD-1 Blockade. *Science* 357 (6349), 409–413. doi:10.1126/science.aan6733

Leblond, F., Davis, S. C., Valdés, P. A., and Pogue, B. W. (2010). Pre-clinical Whole-Body Fluorescence Imaging: Review of Instruments, Methods and Applications. *J. Photochem. Photobiol. B: Biol.* 98 (1), 77–94. doi:10.1016/j.jphotobiol.2009.11.007

Li, L., and Yang, X. (2018). The Essential Element Manganese, Oxidative Stress, and Metabolic Diseases: Links and Interactions. *Oxid Med. Cel Longev* 2018, 7580707. doi:10.1155/2018/7580707

Li, T., Shi, T., Li, X., Zeng, S., Yin, L., and Pu, Y. (2014). Effects of Nano-MnO2 on Dopaminergic Neurons and the Spatial Learning Capability of Rats. *Int. J. Environ. Res. Public Health.* 11 (8), 7918–7930. doi:10.3390/ijerph110807918

Li, M., Zhao, Q., Yi, X., Zhong, X., Song, G., Chai, Z., et al. (2016). Au@MnS@ZnS Core/Shell/Shell Nanoparticles for Magnetic Resonance Imaging and Enhanced Cancer Radiation Therapy. *ACS Appl. Mater. Inter.* 8 (15), 9557–9564. doi:10.1021/acsami.5b11588

Liang, R., Liu, L., He, H., Chen, Z., Han, Z., Luo, Z., et al. (2018). Oxygen-boosted Immunogenic Photodynamic Therapy with Gold Nanocages@manganese Dioxide to Inhibit Tumor Growth and Metastases. *Biomaterials* 177, 149–160. doi:10.1016/j.biomaterials.2018.05.051

Liang, C., Zhang, X., Yang, M., and Dong, X. (2019). Recent Progress in Ferroptosis Inducers for Cancer Therapy. *Adv. Mater.* 31 (51), e1904197. doi:10.1002/adma.201904197

Liu, X., Wang, Q., Zhao, H., Zhang, L., Su, Y., and Lv, Y. (2012). BSA-templated MnO2 Nanoparticles as Both Peroxidase and Oxidase Mimics. *Analyst* 137 (19), 4552–4558. doi:10.1039/c2an35700c

Liu, R., Jing, L., Peng, D., Li, Y., Tian, J., and Dai, Z. (2015). Manganese (II) Chelate Functionalized Copper Sulfide Nanoparticles for Efficient Magnetic Resonance/Photoacoustic Dual-Modal Imaging Guided Photothermal Therapy. *Theranostics* 5 (10), 1144–1153. doi:10.7150/thno.11754

Liu, Y., Bhattarai, P., Dai, Z., and Chen, X. (2019). Photothermal Therapy and Photoacoustic Imaging via Nanotheranostics in Fighting Cancer. *Chem. Soc. Rev.* 48 (7), 2053–2108. doi:10.1039/c8cs00618k

Liu, Y., Xu, J., Liu, L., Tan, J., Gao, L., Wang, J., et al. (2019). Amorphous Manganese Dioxide Coated Polydopamine Nanoparticles for Acid-Sensitive Magnetic Resonance Imaging-Guided Tumor Photothermal Therapy. *J. Biomed. Nanotechnol* 15 (8), 1771–1780. doi:10.1166/jbn.2019.2806

Liu, J., Du, P., Liu, T., Córdova Wong, B. J., Wang, W., Ju, H., et al. (2019). A Black Phosphorus/manganese Dioxide Nanoplatform: Oxygen Self-Supply Monitoring, Photodynamic Therapy Enhancement and Feedback. *Biomaterials* 192, 179–188. doi:10.1016/j.biomaterials.2018.10.018

Liu, Y., Pan, Y., Cao, W., Xia, F., Liu, B., Niu, J., et al. (2019). A Tumor Microenvironment Responsive Biodegradable CaCO3/MnO2- Based Nanoplatform for the Enhanced Photodynamic Therapy and Improved PD-L1 Immunotherapy. *Theranostics* 9 (23), 6867–6884. doi:10.7150/thno.37586

Liu, J., Zhang, W., Kumar, A., Rong, X., Yang, W., Chen, H., et al. (2020). Acridine Orange Encapsulated Mesoporous Manganese Dioxide Nanoparticles to Enhance Radiotherapy. *Bioconjug. Chem.* 31 (1), 82–92. doi:10.1021/acs.bioconjchem.9b00751

Liuyun Gong, L., Zhang, Y., Liu, C., Zhang, M., and Han, S. (2021). Application of Radiosensitizers in Cancer Radiotherapy. *Int. J. Nanomedicine* 16, 1083–1102. doi:10.2147/ijn.s290438

McGranahan, N., Furness, A. J. S., Rosenthal, R., Ramskov, S., Lyngaa, R., Saini, S. K., et al. (2016). Clonal Neoantigens Elicit T Cell Immunoreactivity and Sensitivity to Immune Checkpoint Blockade. *Science* 351 (6280), 1463–1469. doi:10.1126/science.aaf1490

Meng, L., Cheng, Y., Tong, X., Gan, S., Ding, Y., Zhang, Y., et al. (2018). Tumor Oxygenation and Hypoxia Inducible Factor-1 Functional Inhibition via a Reactive Oxygen Species Responsive Nanoplatform for Enhancing Radiation Therapy and Abscopal Effects. *ACS Nano* 12 (8), 8308–8322. doi:10.1021/acsnano.8b03590

Miele, E., Spinelli, G. P., Miele, E., Di Fabrizio, E., Ferretti, E., Tomao, S., et al. (2012). Nanoparticle-based Delivery of Small Interfering RNA: Challenges for Cancer Therapy. *Int. J. Nanomedicine* 7, 3637–3657. doi:10.2147/IJN.S23696

Moghimi, S. M., and Szebeni, J. (2003). Stealth Liposomes and Long Circulating Nanoparticles: Critical Issues in Pharmacokinetics, Opsonization and Protein-Binding Properties. *Prog. Lipid Res.* 42 (6), 463–478. doi:10.1016/s0163-7827(03)00033-x

Nie, Y., Li, D., Peng, Y., Wang, S., Hu, S., Liu, M., et al. (2020). Metal Organic Framework Coated MnO2 Nanosheets Delivering Doxorubicin and Self-Activated DNAzyme for Chemo-Gene Combinatorial Treatment of Cancer. *Int. J. Pharmaceutics* 585, 119513. doi:10.1016/j.ijpharm.2020.119513

Oszlánczi, G., Vezér, T., Sárközi, L., Horváth, E., Kónya, Z., and Papp, A. (2010). Functional Neurotoxicity of Mn-Containing Nanoparticles in Rats. *Ecotoxicol Environ. Saf.* 73 (8), 2004–2009. doi:10.1016/j.ecoenv.2010.09.002

Pfeiffer, D., Pfeiffer, F., and Rummeny, E. (2020). Advanced X-ray Imaging Technology. *Recent Results Cancer Res.* 216, 3–30. doi:10.1007/978-3-030-42618-7_1

Qian, X., Zhang, J., Gu, Z., and Chen, Y. (2019). Nanocatalysts-augmented Fenton Chemical Reaction for Nanocatalytic Tumor Therapy. *Biomaterials* 211, 1–13. doi:10.1016/j.biomaterials.2019.04.023

Rajendrakumar, S. K., Venu, A., Revuri, V., George Thomas, R., Thirunavukkarasu, G. K., Zhang, J., et al. (2019). Hyaluronan-Stabilized Redox-Sensitive Nanoassembly for Chemo-Gene Therapy and Dual T1/T2 MR Imaging in Drug-Resistant Breast Cancer Cells. *Mol. Pharmaceutics* 16 (5), 2226–2234. doi:10.1021/acs.molpharmaceut.9b00189

Razumov, I. A., Zav'yalov, E. L., Troitskii, S. Y., Romashchenko, A. V., Petrovskii, D. V., Kuper, K. E., et al. (2017). Selective Cytotoxicity of Manganese Nanoparticles against Human Glioblastoma Cells. *Bull. Exp. Biol. Med.* 163 (4), 561–565. doi:10.1007/s10517-017-3849-0

Ren, Q., Yang, K., Zou, R., Wan, Z., Shen, Z., Wu, G., et al. (2019). Biodegradable Hollow Manganese/cobalt Oxide Nanoparticles for Tumor Theranostics. *Nanoscale* 11 (47), 23021–23026. doi:10.1039/c9nr07725a

Rich, L. J., Damasco, J. A., Bulmahn, J. C., Kutscher, H. L., Prasad, P. N., and Seshadri, M. (2020). Photoacoustic and Magnetic Resonance Imaging of Hybrid Manganese Dioxide-Coated Ultra-small NaGdF4 Nanoparticles for Spatiotemporal Modulation of Hypoxia in Head and Neck Cancer. *Cancers* 12 (11), 3294. doi:10.3390/cancers12113294

Sárközi, L., Horváth, E., Kónya, Z., Kiricsi, I., Szalay, B., Vezér, T., et al. (2009). Subacute Intratracheal Exposure of Rats to Manganese Nanoparticles: Behavioral, Electrophysiological, and General Toxicological Effects. *Inhal Toxicol.* 21 (Suppl. 1), 83–91. doi:10.1080/08958370902939406

Shah, J., Park, S., Aglyamov, S., Larson, T., Ma, L., Sokolov, K., et al. (2008). Photoacoustic Imaging and Temperature Measurement for Photothermal Cancer Therapy. *J. Biomed. Opt.* 13 (3), 034024. doi:10.1117/1.2940362

Shi, X., and Shen, L. (2018). Integrin α V β 3 Receptor Targeting PET/MRI Dual-Modal Imaging Probe Based on the 64 Cu Labeled Manganese Ferrite Nanoparticles. *J. Inorg. Biochem.* 186, 257–263. doi:10.1016/j.jinorgbio.2018.06.004

Shin, S. W., Jung, W., Choi, C., Kim, S. Y., Son, A., Kim, H., et al. (2018). Fucoidan-Manganese Dioxide Nanoparticles Potentiate Radiation Therapy by Co-targeting Tumor Hypoxia and Angiogenesis. *Mar. Drugs* 16 (12). doi:10.3390/md16120510

Siegel, R. L., Miller, K. D., Fuchs, H. E., and Jemal, A. (2021). Cancer Statistics, 2021. *CA A. Cancer J. Clin.* 71 (1), 7–33. doi:10.3322/caac.21654

Siemer, S., Westmeier, D., Vallet, C., Becker, S., Voskuhl, J., Ding, G.-B., et al. (2020). Retraction of "Resistance to Nano-Based Antifungals Is Mediated by Biomolecule Coronas". *ACS Appl. Mater. Inter.* 12 (13), 15953. doi:10.1021/acsami.9b23592

Singh, P., Kim, Y.-J., Zhang, D., and Yang, D.-C. (2016). Biological Synthesis of Nanoparticles from Plants and Microorganisms. *Trends Biotechnol.* 34 (7), 588–599. doi:10.1016/j.tibtech.2016.02.006

Singh, P., Pandit, S., Mokkapati, V. R. S. S., Garg, A., Ravikumar, V., and Mijakovic, I. (2018). Gold Nanoparticles in Diagnostics and Therapeutics for Human Cancer. *Int. J. Mol. Sci.* 19 (7), 1979. doi:10.3390/ijms19071979

Song, M., Liu, T., Shi, C., Zhang, X., and Chen, X. (2016). Bioconjugated Manganese Dioxide Nanoparticles Enhance Chemotherapy Response by Priming Tumor-Associated Macrophages toward M1-like Phenotype and Attenuating Tumor Hypoxia. *ACS Nano* 10 (1), 633–647. doi:10.1021/acsnano.5b06779

Soratijahromi, E., Mohammadi, S., Dehdari Vais, R., Azarpira, N., and Sattarahmady, N. (2020). Photothermal/sonodynamic Therapy of Melanoma Tumor by a Gold/manganese Dioxide Nanocomposite: *In Vitro* and *In Vivo* Studies. *Photodiagnosis Photodynamic Ther.* 31, 101846. doi:10.1016/j.pdpdt.2020.101846

Siyu Wang, S., You, Q., Wang, J., Song, Y., Cheng, Y., Wang, Y., et al. (2019). MSOT/CT/MR Imaging-Guided and Hypoxia-Maneuvered Oxygen Self-Supply Radiotherapy Based on One-Pot MnO2-mSiO2@Au Nanoparticles. *Nanoscale* 11 (13), 6270–6284. doi:10.1039/c9nr00918c

Tang, H., Li, C., Zhang, Y., Zheng, H., Cheng, Y., Zhu, J., et al. (2020). Targeted Manganese Doped Silica Nano GSH-Cleaner for Treatment of Liver Cancer by Destroying the Intracellular Redox Homeostasis. *Theranostics* 10 (21), 9865–9887. doi:10.7150/thno.46771

Tao, Y., Zhu, L., Zhao, Y., Yi, X., Zhu, L., Ge, F., et al. (2018). Nano-graphene Oxide-Manganese Dioxide Nanocomposites for Overcoming Tumor Hypoxia and Enhancing Cancer Radioisotope Therapy. *Nanoscale* 10 (11), 5114–5123. doi:10.1039/c7nr08747k

Tao Gong, T., Wang, X., Ma, Q., Li, J., Li, M., Huang, Y., et al. (2021). Triformyl Cholic Acid and Folic Acid Functionalized Magnetic Graphene Oxide Nanocomposites: Multiple-Targeted Dual-Modal Synergistic Chemotherapy/photothermal Therapy for Liver Cancer. *J. Inorg. Biochem.* 223, 111558. doi:10.1016/j.jinorgbio.2021.111558

Tarkin, J. M., Ćorović, A., Wall, C., Gopalan, D., and Rudd, J. H. (2020). Positron Emission Tomography Imaging in Cardiovascular Disease. *Heart* 106 (22), 1712–1718. doi:10.1136/heartjnl-2019-315183

Tørring, M. L., Frydenberg, M., Hansen, R. P., Olesen, F., and Vedsted, P. (2013). Evidence of Increasing Mortality with Longer Diagnostic Intervals for Five Common Cancers: a Cohort Study in Primary Care. *Eur. J. Cancer* 49 (9), 2187–2198. doi:10.1016/j.ejca.2013.01.025

Van Allen, E. M., Miao, D., Schilling, B., Shukla, S. A., Blank, C., Zimmer, L., et al. (2015). Genomic Correlates of Response to CTLA-4 Blockade in Metastatic Melanoma. *Science* 350 (6257), 207–211. doi:10.1126/science.aad0095

Wang, C., Guan, Y., Lv, M., Zhang, R., Guo, Z., Wei, X., et al. (2018). Manganese Increases the Sensitivity of the cGAS-STING Pathway for Double-Stranded DNA and Is Required for the Host Defense against DNA Viruses. *Immunity* 48 (4), 675–687. e7. doi:10.1016/j.immuni.2018.03.017

Wang, Z., Zhan, M., Li, W., Chu, C., Xing, D., Lu, S., et al. (2021). Photoacoustic Cavitation-Ignited Reactive Oxygen Species to Amplify Peroxynitrite Burst by

Photosensitization-free Polymeric Nanocapsules. *Angew. Chem. Int. Ed.* 60 (9), 4720–4731. doi:10.1002/anie.202013301

Wen, L., Hyoju, R., Wang, P., Shi, L., Li, C., Li, M., et al. (2021). Hydrogen-Peroxide-Responsive Protein Biomimetic Nanoparticles for Photothermal-Photodynamic Combination Therapy of Melanoma. *Lasers Surg. Med.* 53 (3), 390–399. doi:10.1002/lsm.23292

Wilczewska, A. Z., Niemirowicz, K., Markiewicz, K. H., and Car, H. (2012). Nanoparticles as Drug Delivery Systems. *Pharmacol. Rep.* 64 (5), 1020–1037. doi:10.1016/s1734-1140(12)70901-5

Wu, Q., Lin, Y., Wo, F., Yuan, Y., Ouyang, Q., Song, J., et al. (2017). Novel Magnetic-Luminescent Janus Nanoparticles for Cell Labeling and Tumor Photothermal Therapy. *Small* 13 (39). doi:10.1002/smll.201701129

Xi, J., Da, L., Yang, C., Chen, R., Gao, l., Fan, L., et al. (2017). Mn2+-coordinated PDA@DOX/PLGA Nanoparticles as a Smart Theranostic Agent for Synergistic Chemo-Photothermal Tumor Therapy. *Int. J. Nanomedicine* 12, 3331–3345. doi:10.2147/ijn.s132270

Yang, Y., Shi, H., Wang, Y., Shi, B., Guo, L., Wu, D., et al. (2016). Graphene Oxide/manganese Ferrite Nanohybrids for Magnetic Resonance Imaging, Photothermal Therapy and Drug Delivery. *J. Biomater. Appl.* 30 (6), 810–822. doi:10.1177/0885328215601926

Yang, G., Xu, L., Chao, Y., Xu, J., Sun, X., Wu, Y., et al. (2017). Hollow MnO2 as a Tumor-Microenvironment-Responsive Biodegradable Nano-Platform for Combination Therapy Favoring Antitumor Immune Responses. *Nat. Commun.* 8 (1), 902. doi:10.1038/s41467-017-01050-0

Yang, R., Hou, M., Gao, Y., Lu, S., Zhang, L., Xu, Z., et al. (2019). Biomineralization-inspired Crystallization of Manganese Oxide on Silk Fibroin Nanoparticles for *In Vivo* MR/fluorescence Imaging-Assisted Tri-modal Therapy of Cancer. *Theranostics* 9 (21), 6314–6333. doi:10.7150/thno.36252

Yang, M., Li, J., Gu, P., and Fan, X. (2021). The Application of Nanoparticles in Cancer Immunotherapy: Targeting Tumor Microenvironment. *Bioactive Mater.* 6 (7), 1973–1987. doi:10.1016/j.bioactmat.2020.12.010

Yao, Y., Li, P., He, J., Wang, D., Hu, J., and Yang, X. (2021). Albumin-Templated Bi2Se3-MnO2 Nanocomposites with Promoted Catalase-like Activity for Enhanced Radiotherapy of Cancer. *ACS Appl. Mater. Inter.* 13 (24), 28650–28661. doi:10.1021/acsami.1c05669

Yin, Z., Ji, Q., Wu, D., Li, Z., Fan, M., Zhang, H., et al. (2021). H2O2-Responsive Gold Nanoclusters @ Mesoporous Silica @ Manganese Dioxide Nanozyme for "Off/On" Modulation and Enhancement of Magnetic Resonance Imaging and Photodynamic Therapy. *ACS Appl. Mater. Inter.* 13 (13), 14928–14937. doi:10.1021/acsami.1c00430

Yidan Wang, Y., Song, S., Lu, T., Cheng, Y., Song, Y., Wang, S., et al. (2019). Oxygen-supplementing Mesoporous Polydopamine Nanosponges with WS2 QDs-Embedded for CT/MSOT/MR Imaging and Thermoradiotherapy of Hypoxic Cancer. *Biomaterials* 220, 119405. doi:10.1016/j.biomaterials.2019.119405

Yijue Wang, Y., Zou, L., Qiang, Z., Jiang, J., Zhu, Z., and Ren, J. (2020). Enhancing Targeted Cancer Treatment by Combining Hyperthermia and Radiotherapy Using Mn-Zn Ferrite Magnetic Nanoparticles. *ACS Biomater. Sci. Eng.* 6 (6), 3550–3562. doi:10.1021/acsbiomaterials.0c00287

Yuan, X., Yin, Y., Zan, W., Sun, X., and Yang, Q. (2019). Hybrid Manganese Dioxide-Bovine Serum Albumin Nanostructure Incorporated with Doxorubicin and IR780 for Enhanced Breast Cancer Chemo-Photothermal Therapy. *Drug Deliv.* 26 (1), 1254–1264. doi:10.1080/10717544.2019.1693706

Zaimy, M. A., Saffarzadeh, N., Mohammadi, A., Pourghadamyari, H., Izadi, P., Sarli, A., et al. (2017). New Methods in the Diagnosis of Cancer and Gene Therapy of Cancer Based on Nanoparticles. *Cancer Gene Ther.* 24 (6), 233–243. doi:10.1038/cgt.2017.16

Zanzonico, P. B. (2019). Benefits and Risks in Medical Imaging. *Health Phys.* 116 (2), 135–137. doi:10.1097/hp.0000000000001038

Zhan, Y., Shi, S., Ehlerding, E. B., Graves, S. A., Goel, S., Engle, J. W., et al. (2017). Radiolabeled, Antibody-Conjugated Manganese Oxide Nanoparticles for Tumor Vasculature Targeted Positron Emission Tomography and Magnetic Resonance Imaging. *ACS Appl. Mater. Inter.* 9 (44), 38304–38312. doi:10.1021/acsami.7b12216

Zhang, M., Cao, Y., Wang, L., Ma, Y., Tu, X., and Zhang, Z. (2015). Manganese Doped Iron Oxide Theranostic Nanoparticles for Combined T1 Magnetic Resonance Imaging and Photothermal Therapy. *ACS Appl. Mater. Inter.* 7 (8), 4650–4658. doi:10.1021/am5080453

Zhao, Z., Zhou, Z., Bao, J., Wang, Z., Hu, J., Chi, X., et al. (2018). Octapod Iron Oxide Nanoparticles as High-Performance T_2 Contrast Agents for Magnetic Resonance Imaging. *Nat. Commun.* 4 (3), 2266. doi:10.1038/ncomms3266

Zhao, H., Wang, J., Li, X., Li, Y., Li, C., Wang, X., et al. (2021). A Biocompatible Theranostic Agent Based on Stable Bismuth Nanoparticles for X-ray Computed Tomography/magnetic Resonance Imaging-Guided Enhanced Chemo/photothermal/chemodynamic Therapy for Tumours. *J. Colloid Interf. Sci.* 604, 80–90. doi:10.1016/j.jcis.2021.06.174

Zhi, D., Yang, T., O'Hagan, J., Zhang, S., and Donnelly, R. F. (2020). Photothermal Therapy. *J. Controlled Release* 325, 52–71. doi:10.1016/j.jconrel.2020.06.032

Zhu, W., Liu, K., Sun, X., Wang, X., Li, Y., Cheng, L., et al. (2015). Mn2+-doped Prussian Blue Nanocubes for Bimodal Imaging and Photothermal Therapy with Enhanced Performance. *ACS Appl. Mater. Inter.* 7 (21), 11575–11582. doi:10.1021/acsami.5b02510

Zhu, J., Li, H., Xiong, Z., Shen, M., Conti, P. S., Shi, X., et al. (2018). Polyethyleneimine-Coated Manganese Oxide Nanoparticles for Targeted Tumor PET/MR Imaging. *ACS Appl. Mater. Inter.* 10 (41), 34954–34964. doi:10.1021/acsami.8b12355

Zhu, Y., Shi, H., Li, T., Yu, J., Guo, Z., Cheng, J., et al. (2020). A Dual Functional Nanoreactor for Synergistic Starvation and Photodynamic Therapy. *ACS Appl. Mater. Inter.* 12 (16), 18309–18318. doi:10.1021/acsami.0c01039

Conflict of Interest: The authors declare that the research was conducted in the absence of any commercial or financial relationships that could be construed as a potential conflict of interest.

Publisher's Note: All claims expressed in this article are solely those of the authors and do not necessarily represent those of their affiliated organizations, or those of the publisher, the editors and the reviewers. Any product that may be evaluated in this article, or claim that may be made by its manufacturer, is not guaranteed or endorsed by the publisher.